Temperature dependence of the Raman modes in $LiNbO_3$ and mechanism of the phase transition

A. Ridah,* M. D. Fontana, and P. Bourson†
Laboratoire Matériaux Optiques à Propriétés Spécifiques, CLOES, University of Metz and Supelec, 2 rue E. Belin, 57078 Metz Cedex 3, France
(Received 27 February 1997)

We have performed Raman-scattering measurements on $LiNbO_3$ as a function of temperature. In the configuration (ZZ) both a soft phonon A_1 (TO) and a quasielastic scattering have been observed and carefully analyzed within a model including a decoupled damped oscillator and a Debye relaxation mode. Good agreement was achieved in the dielectric constant between the calculated values deduced from Raman studies and the experimental data reported by Tomeno and Matsumara. This agreement proves the validity of our fitted phonon parameters and supports the mainly order-disorder character for the ferroelectric-paraelectric phase transition of $LiNbO_3$. [S0163-1829(97)05533-1]

I. INTRODUCTION

Lithium niobate (LN) is a well-known material for applications in nonlinear optics, optoelectronics, and acoustics. Surprisingly, the mechanism of the structural phase transition from the paraelectric to the ferroelectric phase occurring around 1400 K is not clearly elucidated and is still the object of controversy despite several investigations. By means of the Raman-scattering measurements a softening of a phonon mode of A_1 symmetry was observed in the whole temperature range up to the Curie temperature.[1,2] In contradiction with this soft-mode picture, Okamoto, Wang, and Scott[3] have shown that the lowest frequency phonon is nearly constant in frequency and highly damped but is coupled with a quasielastic scattering. Therefore they concluded that the phase transition in $LiNbO_3$ should be described rather by an order-disorder picture than by a displacive mechanism.

A valuable way to discriminate between both these views is to compare the dielectric permittivity measured at low frequency ε (exp) and the value of the dielectric constant calculated from optical-phonon frequencies ε (calc). Recently, Tomeno and Matsumara[4] showed that ε (calc) derived from results reported by Okamoto, Wang, and Scott[3] significantly deviates at high temperatures, from their dielectric data. On the contrary, their data are closer to the value ε (calc) deduced from Raman measurements of Johnston and Kaminow,[1] although a complete agreement between ε (calc) and ε (exp) was not achieved in the whole temperature range. In the present study we show that, by means of Raman-scattering results, we are able to reconcile the dielectric data obtained at low frequency with values of the dielectric permittivity derived from the optical-phonon measurements.

In this Raman investigation we pay careful attention to obtaining meaningful information, both directly from experimental features and indirectly from a model. The confidence on the parameter values derived from model calculations, and thus the validity of the model, depend on their reliability with the information which is deduced from other techniques.

Compared with the previous paper of Okamoto, Wang, and Scott[3] we point out the differences as follows in our study: (i) we measure the temperature dependence of the A_1 spectrum in the whole frequency range from 0 up to 900 cm^{-1}, (ii) we study the possible existence of the quasielastic scattering (QES) in various configurations, (iii) we use a simpler and more realistic model, (iv) we discuss the reliability of our results with other results which were independently obtained, specially by dielectric measurements.

II. EXPERIMENTAL RESULTS

A. Room temperature

At room temperature an assignment of the Raman peaks to the optical phonons in $LiNbO_3$ was recently established from measurements of function compositions.[5] This allows us to remove some ambiguities in the Raman spectra previously reported. The A_1 (TO) spectrum recorded at room temperature in the $X(ZZ)Y$ configuration is shown in Fig. 1. As expected according to the group theory, four peaks are detected and are lying around 252, 275, 332, and 632 cm^{-1}. They are denoted, respectively, A_1 (TO_1), A_1 (TO_2), A_1 (TO_3), and A_1 (TO_4). A shoulder of the A_1 (TO_4) peak is additionally visible in the spectrum. This scattering around 700 cm^{-1} is probably caused by two-phonon density of states as shown in Ref. 5.

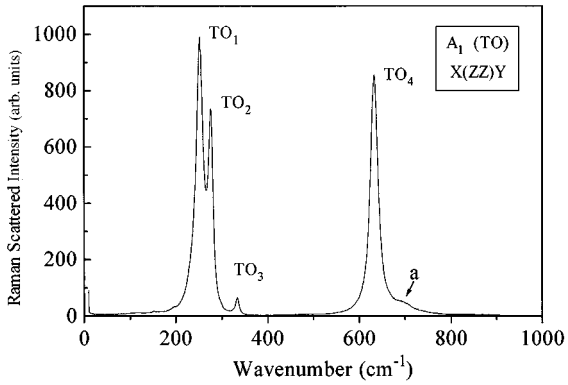

FIG. 1. Raman $X(ZZ)Y$ spectrum recorded at room temperature in a nearly stoichiometric $LiNbO_3$ crystal. It shows four A_1 (TO) first-order phonon peaks and a second-order phonon band (a).

At 300 K our results are similar to those previously reported, excepted for A_1 (TO_3) which was not detected by Okamoto, Wang, and Scott.[3] It is known that some of the properties of LN are dependent on the stoichiometric defects.[6,7] Whereas the phonon frequency exhibits only a small dependence on the composition of the crystal, the phonon damping is very sensitive to it.[5] As shown by Scott and Burns[8] this variation even constitutes a tool to determine the composition variation in LN, from the congruent sample to the stoichiometric one.[9,5] Even if we are not directly concerned by it in the present study, the existence of intrinsic defects related to the nonstoichiometry of the crystal could lead to an erroneous interpretation of the quasielastic scattering, if any. Therefore, among several pure LN samples, we have chosen for our investigation, the crystal, the composition of which is closer to the stoichiometry ($x_c = 49.74\%$). This composition $x_c = [\mathrm{Li}]/[\mathrm{Li}]+[\mathrm{Nb}]$ was determined by means of our calibration curve from the measurement of the linewidth of the lowest frequency E (TO) phonon.[5] This line is usually considered for this calculation since it is intense and well resolved. Its damping is known to decrease when the concentration of intrinsic defects diminishes, and thus the stoichiometric composition ($x_c = 50\%$) approaches.

Therefore we note an apparent contradiction in the investigation of Okamoto, Wang, and Scott,[3] since the damping of the soft mode was found to be larger in the ''stoichiometric'' sample ($13\ \mathrm{cm}^{-1}$) than in the ''congruent'' sample ($11\ \mathrm{cm}^{-1}$) whereas we obtain $9.8\ \mathrm{cm}^{-1}$ from our data reported in Fig. 1 for a crystal very close to the stoichiometric composition.

B. Temperature dependence

We follow the temperature dependence of the A_1 spectrum in the whole frequency range, and not only in the lowest part. Indeed, all optical phonons can, in principle, contribute to the dielectric properties. Figure 2 exhibits the A_1 (TO) spectrum recorded for various temperatures up to 1100 K.

Several features can be directly deduced from the observation of this temperature dependence. Well resolved at 300 K, the two lowest frequency peaks are nearly indiscernable at 579 and 703 K. For temperatures larger than 800 K a shoulder appears in the low-frequency side of the most intense peak. This means that when the temperature increases, the second mode which decreases in frequency pushes down the lowest mode. This anticrossing of the two lowest modes is accompanied by an energy transfer between them. At higher temperatures, above 900 K both peaks are again clearly distinct and their separation becomes larger and larger when the temperature continues to increase, so that the lowest mode is peaked around $165\ \mathrm{cm}^{-1}$ at 1100 K, reflecting thus a large mode softening. It is also remarkable that all four A_1 (TO) modes are resolved at 1100 K, despite their large broadening and the high temperature.

Beside the mode softening, we observe the clear appearance of a quasielastic scattering (QES) in the tail of the Rayleigh line, for temperature above 700 K. This feature will be discussed in more detail below.

If we now pay attention to the very high-frequency range of the A_1 spectrum [see Fig. 2(b)] and its thermal behavior,

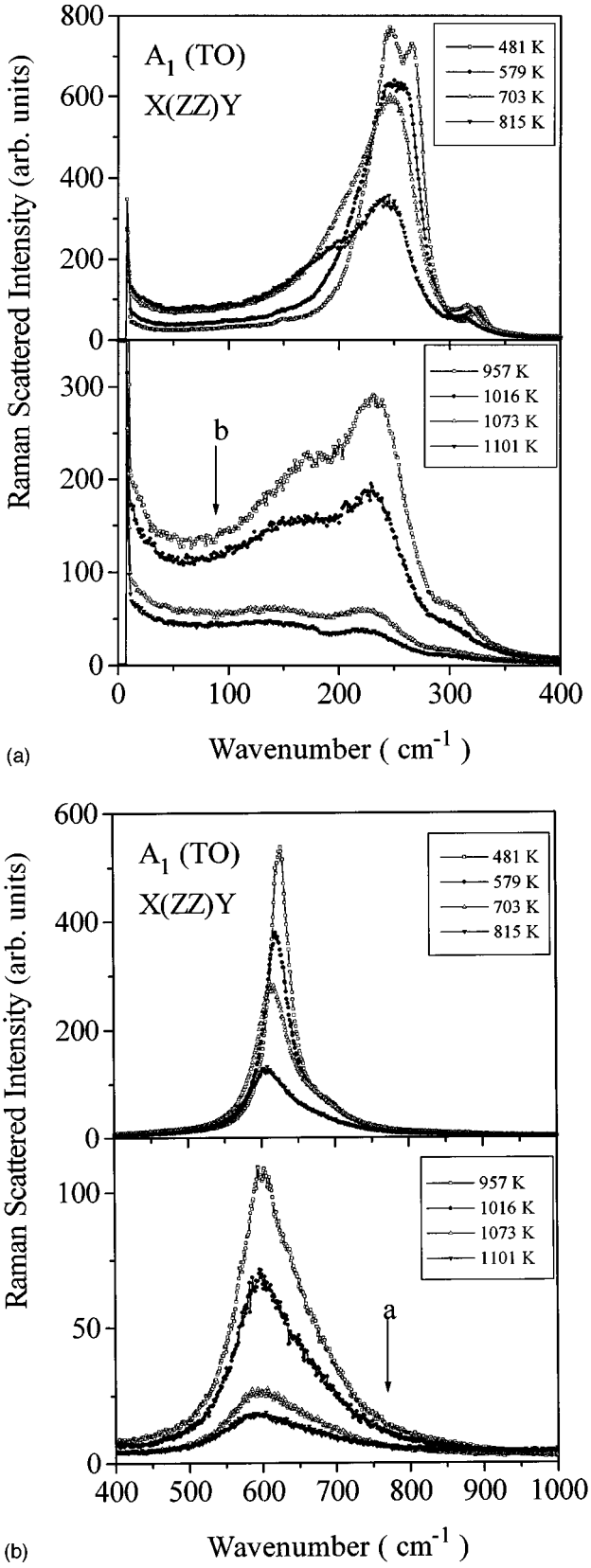

FIG. 2. Temperature dependence of the $X(ZZ)Y$ spectrum. Scattered intensity appearing at low frequency for temperatures above 700 K is the tail of a quasielastic scattering. The arrows mark the second-order phonon bands (a) and (b) which occur at high temperatures.

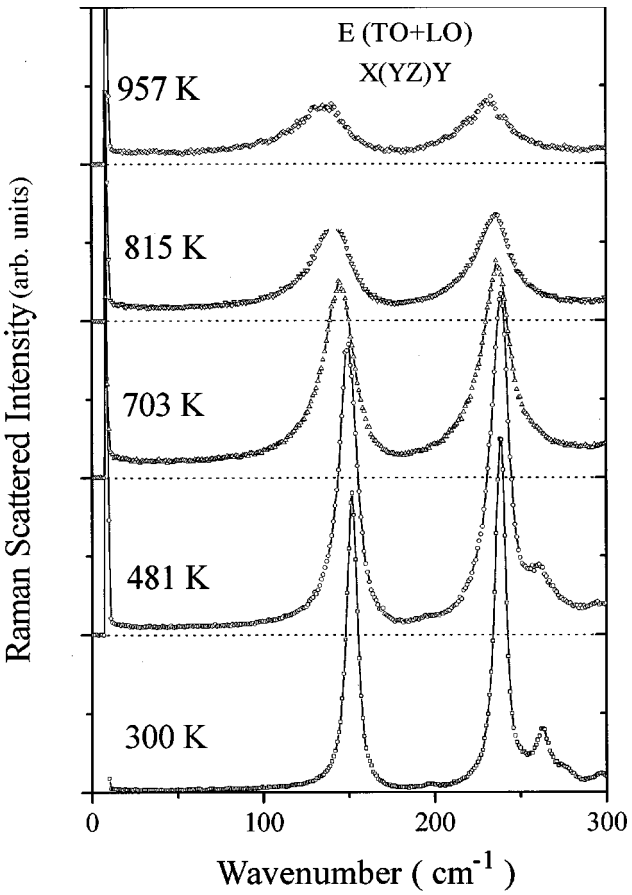

FIG. 3. Temperature dependence of the $X(YZ)Y$ Raman spectrum. We note the large broadening of the lines without apparent shifts in frequency.

we note that the shoulder (a) of the fourth A_1 (TO_4) peak possesses a relative intensity which becomes larger and larger compared with the A_1 (TO_4) intensity as the temperature increases. This corroborates that the peak (lying around 696 cm^{-1} at room temperature) originates from the two-phonon density of states. Above 900 K, another band denoted (b) [see Fig. 2(a)] which is unexpected according to the group theory, occurs at low frequency between the QES and the soft-phonon peak. This scattered intensity extending from 40 up to 100 cm^{-1}, is nearly absent in the spectrum at low temperature. Since its intensity seemingly increases likewise as the band (a) around 700 cm^{-1}, it can be attributed to a similar process. As shown in Ref. 5 the temperature dependence of the intensity of the broadbands (a) and (b) prove that they originate from a second-order process. The presence of such an intense two-phonon scattering is in fact a characteristic of the Raman spectrum in the oxide crystals[10,11] and is induced by the large polarizability of the oxygen ion, as shown by Migoni, Bilz, and Bäuerle[11] by means of lattice-dynamical calculations. Moreover this scattering can be strongly affected by nonstoichiometric defects which break the Raman selection rules.[5]

Now we turn to the thermal behavior of the spectrum recorded in $X[YZ]Y$ corresponding to the detection of the E (TO) and E (LO) phonons (Fig. 3). As the temperature increases the lowest phonons shift down slowly but rapidly broaden. The behavior of the E spectrum usually merits less

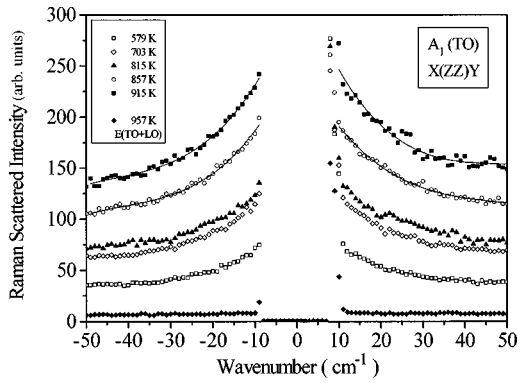

FIG. 4. Temperature dependence of the quasielastic scattering in the $X(ZZ)Y$ configuration. The low-frequency spectrum recorded in the $X(YZ)Y$ configuration is nearly temperature independent (see Fig. 3). The comparison points out the anisotropic character of the quasielastic scattering.

interest than that of the A_1 spectrum because it is related to the smaller dielectric constant $\varepsilon_a < \varepsilon_c$. The nearly temperature independence of the E (TO) phonon frequency is consistent with the nearly constant value of ε_a with temperature.[4] It is the reason for which more attention is devoted below to the analysis of the A_1 spectrum.

We come back to the QES and we compare in Fig. 4 the behavior of the QES carried out in the A_1 and E spectra, respectively. In the (ZZ) spectrum, the QES can be unambiguously discerned from the Rayleigh scattering by the broadening of the tail in both sides of the Rayleigh line. The intensity of this scattering increases with temperature. In contrast with the (ZZ) spectrum, the (YZ) spectrum displays, in the same experimental conditions, at low frequency only the elastic scattering which is nearly independent of temperature.

This means that the QES and the relaxation process related to it, are largely anisotropic: it does exist along the ferroelectric axis only which corresponds to the A_1 phonon polarization. In addition we note that there is no intensity transfer between the soft-phonon peak and the QES. Both intensities increase simultaneously with temperature. We summarize the main features derived from the experimental data. The temperature dependence of the A_1 (TO) spectrum shows the coexistence of a large phonon softening and a quasielastic scattering. Since all one- or two-phonon peaks, as well as the QES, can be clearly discerned and assigned, the results thus do not suffer any ambiguity and will be confirmed below by the analysis of the data with an appropriate model. Spectra reported by Okamoto, Wang, and Scott,[3] seem to be of lower quality and the peaks less resolved than our spectra. Moreover the signal (b), was erroneously attributed to a leakage of the E phonon. Indeed no scattered intensity is detected below 100 cm^{-1} in the E (TO) spectrum. We thus estimate that the band (b) should not be neglected in the fitting procedure, particularly at high temperatures.

III. MODEL

As usual, the Raman scattered intensity can be written in terms of the imaginary part of the dielectric permittivity, as

$$I(\omega)=K[n(\omega)+1]\varepsilon''(\omega), \tag{1}$$

where $n(\omega)+1$ is the Bose-Einstein population factor for the Stokes scattering, and K is a proportionality factor. K depends on various experimental conditions, like the laser power, the characteristics of the used optical components, the spectrometer, and the amplifier together with the characteristics of the crystal, such as the crystal absorption. It is therefore difficult to explicitly calculate. As it is a constant for all modes, for a given temperature and a scattering geometry, K is deduced from the fit calculations.

As the various peaks are discerned in the A_1 (TO) spectrum, we consider that the dielectric response arises from the simple superposition of damped harmonic oscillators and a Debye relaxation to describe the phonon peaks and the QES, respectively. Indeed there is no experimental indication for any intensity transfer or coupling between peaks. We therefore write the phonon dielectric response as

$$\varepsilon_i(\omega)=\Delta\varepsilon_i\omega_{\mathrm{TO}i}^2(\omega_{\mathrm{TO}i}^2-\omega^2-j\omega\gamma_i)^{-1}, \tag{2}$$

and the relaxation response as

$$\varepsilon_r(\omega)=\Delta\varepsilon_r(1+j\omega\tau)^{-1}, \tag{3}$$

where $\omega_{\mathrm{TO}i}$, γ_i, and $\Delta\varepsilon_i$ are, respectively, the frequency, the damping, and the oscillator strength of the ith TO phonon, while $\Delta\varepsilon_r$ and τ are the relaxation strength and the relaxation time. In the fitting procedure, there are the factors $K\Delta\varepsilon_i=\alpha_i$ for each phonon and $K\Delta\varepsilon_r=\alpha_r$ for the relaxator, which are in fact adjusted. This means that, in principle, the oscillator strength is calculated independently of the fit of the Raman spectra from the LO-TO splitting as

$$S_i=\varepsilon_\infty\left[\left(\frac{\omega_{\mathrm{LO},i}}{\omega_{\mathrm{TO},i}}\right)^2-1\right]\prod_{k\neq i}\frac{\omega_{\mathrm{LO}k}^2-\omega_{\mathrm{TO}i}^2}{\omega_{\mathrm{TO}k}^2-\omega_{\mathrm{TO}i}^2}, \tag{4}$$

where ε_∞ is the dielectric constant at optical frequencies taken as the square of the refractive index.

This method thus needs the knowledge of all LO and TO frequencies at each temperature. The sign and the value of the strength S_i depend both on the assignment of the TO-LO frequencies of each phonon. On the contrary, the sum denoted S of all S_i does not depend on the model and therefore is characteristic of the permittivity. We can use this quantity S as the sum of S_i deduced from Eq. (4), to indirectly determine the oscillator strength $\Delta\varepsilon_i$ with each phonon from the fitting of the Raman spectra. We proceed as follows. At each temperature, we obtain by adjustment of the spectrum the quantities $\omega_{\mathrm{To}i}$, γ_i, and α_i for each phonon together with τ and α_r. As we have $\Sigma\alpha_i=K\Sigma\Delta\varepsilon_i=KS$, we deduce the constant K for each temperature as $K=\Sigma\alpha_i/S$. Then we derive the oscillator strength for each phonon and the relaxator strength $\Delta\varepsilon_r=\alpha_r/K$. The quantity $\Delta\varepsilon$ ($\Delta\varepsilon_r$) is really the contribution to the dielectric constant of the phonon (relaxator). Indeed $\Delta\varepsilon_i$ can be deduced from the integration of the modified integrated intensity via the Kramers-Kronig relationship:

$$\frac{2}{K\pi}\int_b^a\frac{I(\omega)}{\omega[n(\omega)+1]}=\frac{2}{\pi}\int_b^a\frac{\varepsilon''(\omega)}{\omega}=\Delta\varepsilon, \tag{5}$$

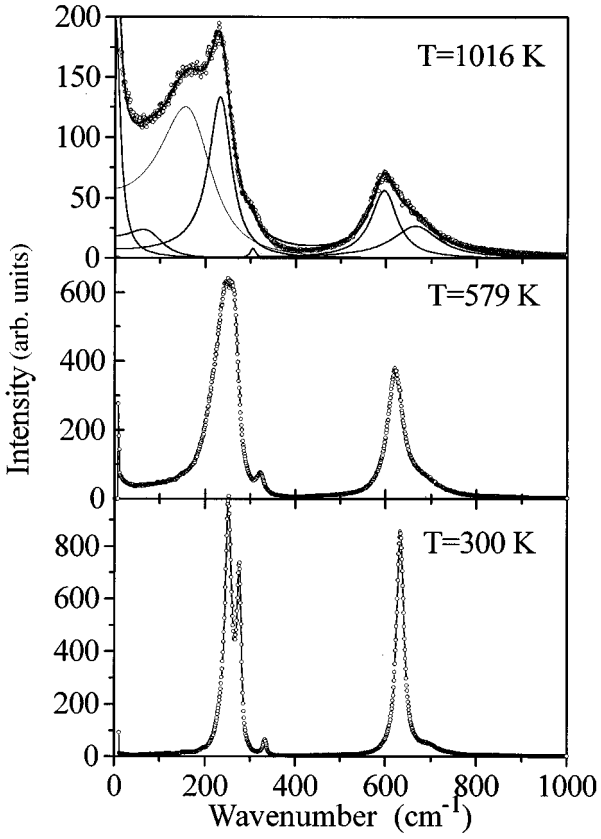

FIG. 5. Three examples of the agreement which is achieved between experimental (circle points) and calculated spectra (lines).

where a and b are the low- and high-frequency limits of the phonon peak.

IV. ANALYSIS OF THE RESULTS AND DISCUSSION

We fit the A_1 (TO) Raman-scattered intensity to Eq. (1) with $\varepsilon(\omega)$ given by Eq. (2) or Eq. (3) in the whole frequency range (10–1000 cm^{-1}). As the spectrum was recorded in the same experimental conditions for all temperatures, we can thus obtain the thermal behavior of all characteristics of each phonon (frequency, damping, and strength) and of the relaxator (time and strength). These last parameters are determined with a larger confidence if low-frequency data in both sides of the Rayleigh line (see Fig. 4) are considered. Some examples of the agreement which is achieved between experimental and calculated spectra are reported in Fig. 5.

Figure 6 displays the temperature dependence of the frequency and damping of the lowest A_1 (TO) modes. It is clearly seen that the lowest mode exhibits a large softening with increasing temperature from the value 252 cm^{-1} at room temperature down to 160 cm^{-1} at 1100 K.

Simultaneously its damping hugely increases so that the soft mode becomes highly damped ($\gamma/\omega\approx1$) at 1100 K. The characteristics of the second mode A_1 (TO_2) follow similar but less pronounced thermal behaviors as those of the A_1 (TO_1) mode. The A_1 (TO_2) behavior is usual for each normal phonon mode, owing to the dilatation of the unit cell and the increase of anharmonicity with the temperature.

It is to be noted that in Fig. 6, we have chosen to represent as continuous the characteristics (damping and frequency) of

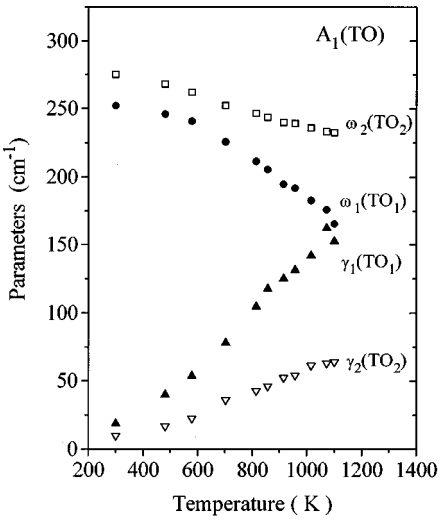

FIG. 6. Temperature dependence of the phonon ω and damping γ for the two lowest A_1 (TO) phonons, as deduced by the fit.

the two lowest modes. This originates from an anticrossing occurring between them when the temperature increases. The A_1 (TO_2) phonon softens more rapidly than the A_1 (TO_1) mode and then pushes it down to lower frequencies. This implies that the ionic motions associated with the A_1 (TO_1) and A_1 (TO_2) modes are transferred to each other. Figure 7 shows the temperature dependence of the frequency and damping of the A_1 (TO_3) and A_1 (TO_4) phonons. As for the A_1 (TO_2), the parameters exhibit the thermal behavior expected for a phonon with increasing temperature.

The temperature dependence of the strength for the phonons and the relaxator is shown in Fig. 8. The oscillator strengths of the A_1 (TO_3) and A_1 (TO_4) modes are small and nearly constant in the whole temperature range. The strength $\Delta\varepsilon_2$ of the A_1 (TO_2) phonon is small up to 600 K, then exhibits an increase and reaches a nearly constant value between 900 and 1100 K. The strengths of the soft mode and

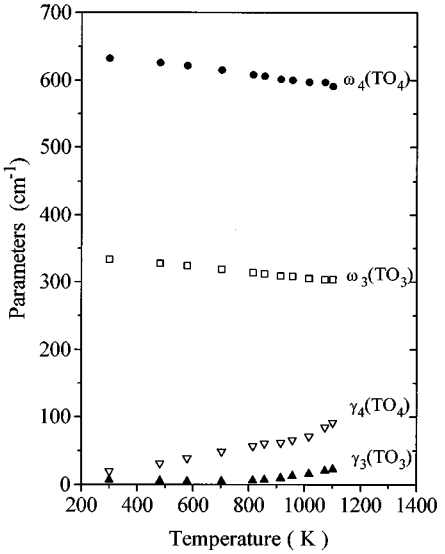

FIG. 7. Temperature dependence of the phonon ω and damping γ for the two highest A_1 (TO) phonons, as deduced by the fit.

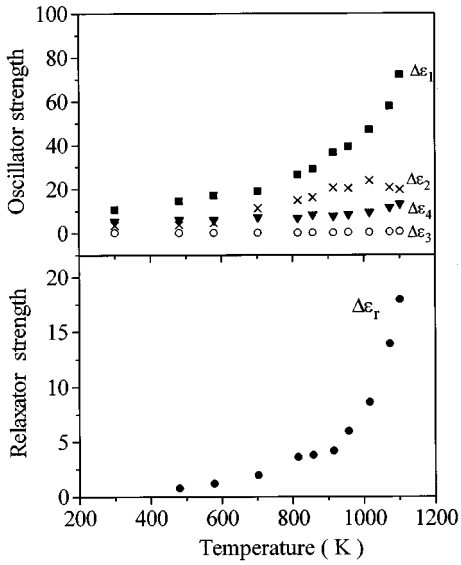

FIG. 8. Temperature dependence of the oscillator strength $\Delta\varepsilon$ for each A_1 (TO) phonon and for the relaxation mode. Note the change in the scale.

the relaxation mode display similar thermal behaviors. They both increase nicely with increasing temperature up to 900 K, and then more quickly on approaching the phase transition. It is necessary to note the differences in the magnitudes of the strengths S_r, $\Delta\varepsilon_1$, and $\Delta\varepsilon_2$. At 1100 K, $\Delta\varepsilon_2$ and S_r have nearly the same values (equal to 17), just above the value of $\Delta\varepsilon_1$ at room temperature. Therefore it is clear that the soft-mode strength is preponderant in the whole temperature range, even if the relaxator strength considerably increases at high temperatures.

Now we discuss the temperature dependence of the ''last'' parameter derived from the fit, i.e., the relaxation time. As shown in Fig. 9, the inverse relaxation time displays a critical slowing down with increasing temperature. The fit of the values of τ^{-1} to $\tau^{-1}=\tau_0^{-1}\ (T_0-T)/T_0$ yields $\tau_0^{-1}=53\ \mathrm{cm}^{-1}$ and $T_0=1310$ K. We note the relatively large values of τ^{-1} or τ_0^{-1}, which are comparable to the usual values of the soft-mode frequency. This is consistent with the detection of the relaxation processes by means of Raman scattering in the low-frequency phonon frequency range. It is interesting to compare the $\tau^{-1}(T)$ plot with the temperature dependence of the soft-mode frequency squared, reported in the same figure. The plot of $\omega^2_{TO_1}(T)$ is extrapolated to zero at a temperature much larger than $T_0=1310$ K. This means that, even if the soft mode and relaxation processes both contribute to the mechanism of the phase transition, the relaxation mode is finally dominant to drive it.

In fact, this description of the transition mechanism assumes that no additional process exists at a frequency still lower than the relaxation mode frequency. In other terms, it is necessary to check if the dielectric permittivity ε_3 reproduces the values and the thermal behavior of the dielectric data as measured at low frequency along the z axis. For this, we calculate the values of ε (calc), as the sum of the relaxation ($\Delta\varepsilon_r$), phonon ($\Delta\varepsilon_i$), and electronic (ε_∞) contributions.

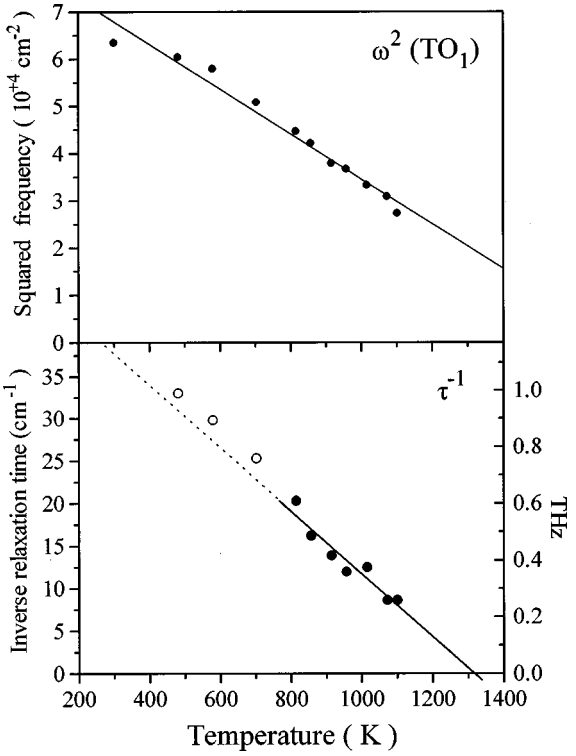

FIG. 9. Temperature dependence of the soft-phonon frequency squared and the inverse relaxation time. Full symbols denote values of τ^{-1} which are deduced from the fits with a large confidence.

$$\varepsilon \ \ (\text{calc}) = \Delta\varepsilon_r + \Sigma\Delta\varepsilon_i + \varepsilon_\infty = \Delta\varepsilon_r + \varepsilon_{\text{lat}}, \qquad (6)$$

where ε_{lat} is the lattice contribution to ε. This relationship allows us to rely on ε (calc) and the measured value ε (exp), even if an extradispersion exists between piezoresonances and the lowest optical-phonon frequency. This is not possible with the value of εprovided by the Lyddane-Sachs-Teller (LST) relation, ε (LST), which in fact is equal to ε_{lat}. Our values ε (calc) can be compared with the experimental values ε (exp) as measured by Tomeno and Matsumara[4] at frequencies (10 MHz) above piezoresonances, i.e., the clamped dielectric constant. The crystal used in their experiments concerned a congruent sample ($x_C = 48.74\%$), with a Curie temperature T_C (exp)=1410 K.[4] Therefore it could be considered as suspicious to compare their results with the Raman data obtained in a sample with a different composition ($x_C = 49.7\%$). In fact in the temperature range (300–1100 K) which corresponds to the relatively small values of ε (from 26 up to 128), the absolute change due to the composition is very small. Probably this variation is much stronger in the vicinity of T_C when ε_3 is larger, which should partly reflect the dependence of T_C on the crystal composition.[12] Therefore, in the temperature range 300–1100 K covered by our Raman studies, we think the comparison between our results and the data of Tomeno Matsumara is valid.[4]

Figure 10 shows the temperature dependence of both ε (calc), and ε (exp), and points out the remarkable agreement between these values in the whole temperature range. It is necessary to remember that values ε (calc) and ε (exp) are obtained by separate and completely independent ways. This important result proves that no extra dispersion exists between 10 MHz and the frequency characterizing the relaxation process evidenced by the quasielastic scattering, and confirms that this relaxation mode triggers the phase transitions in $LiNbO_3$ (Fig. 9). It can be underlined that the ε (exp) can also be reproduced according to the Kramers-Kronig relation [see Eq. (5)] in integrating directly the experimental scattered intensity in the whole frequency range.

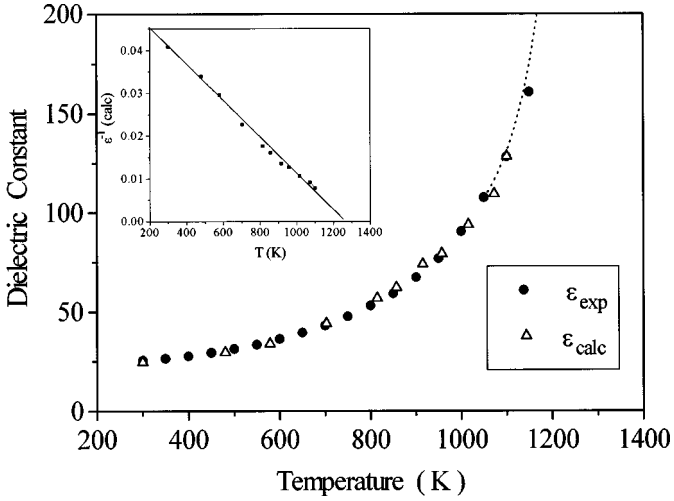

FIG. 10. Temperature dependence of the dielectric permittivity along the c axis. The values ε (calc) are deduced from our Raman results via Eq. (6) whereas ε (exp) represents the direct data obtained by Tomeno and Matsumara (Ref. 4) at 10 MHz. Inset: Temperature dependence of ε^{-1} (calc).

Consistent with the agreement achieved between ε (exp) and ε (calc) as deduced from Eq. (6), the lattice contribution ε (lat), which is equal to ε (exp) for temperatures between 300 and 700 K, is unable to reproduce ε (exp) for higher temperatures. The soft-phonon contribution is dominant in the noncritical temperature range only. Similar results were reported in other oxydic ferroelectrics such as $KNbO_3$ (Ref. 13) and $BaTiO_3$.[14]

Another interesting result is reported in the inset of Fig. 10. The reciprocal calculated dielectric constant shows a linear decrease ε^{-1} (calc) $\alpha C(T_0^* - T)$ with $T_0^* = 1260$ K. This value is very close to that derived from the plot $\tau^{-1}(T)$: $T_0 = 1310$ K and confirms the interpretation of the phase-transition mechanism as given above, since ε (calc) takes into account of the relaxation mode contribution. The agreement achieved between the experimental dielectric data and the calculated values in the whole temperature range proves also the validity of the model used to obtain the parameter values entering the calculation of ε (calc).

The choice of a suitable model is of great importance for the analysis of the experimental data even if the Raman spectra recorded in LN versus temperature do not exhibit significant changes among authors. Indeed, whereas a good agreement is achieved between ε (exp) and our values ε (calc), it was shown in Ref. 4 that the results obtained by Okamoto, Wang, and Scott[3] disagree with ε (exp) in the whole temperature range, and those reported by Johnston and Kaminow[1] are closer to ε (exp), but significantly deviate from ε (exp) for temperatures larger than 800 K.

These results were obtained assuming a coupled relaxator-phonon response function and a purely soft-phonon response, respectively, to fit the Raman data. On the con-

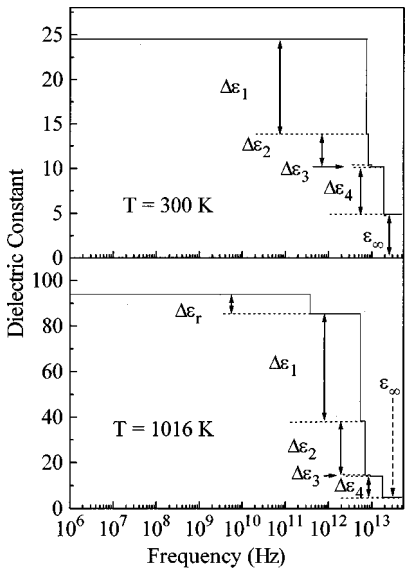

FIG. 11. Frequency dielectric behavior of $LiNbO_3$ at two extreme temperatures (schematic picture). In each temperature the contributions arising from phonons, electrons, and relaxation mode are indicated. Note the change in the scale between the upper and lower parts.

trary, based on the simple coexistence of a soft-phonon and a relaxation mode without any coupling, our model is the only one which is able to reproduce the experimental dielectric behavior. Consequently, we describe the dielectric dispersion in the whole frequency range above piezoresonances and its variation with temperature. This frequency dependence of ε is shown in Fig. 11 for two extreme temperatures. This figure points out the absence of any low-frequency dispersion below the relaxation mode and shows the contributions of various processes to the dielectric permittivity and their changes with temperature.

Now we can point out the differences between our results and those previously reported by Okamoto, Wang, and Scott.[3] In their paper both A_1 (TO_1) and A_1 (TO_2) phonons are nearly constant in frequency whereas the damping of the A_1 (TO_2) mode is exceptionally large. In our opinion, the model proposed by these authors is unrealistic and thus leads to an erroneous interpretation. Indeed there is no argument to invoking a coupling between the QES and the lowest frequency phonon, since experimental data do not give any evidence of a transfer of intensity or strength between the corresponding peaks. This model therefore leads to a picture of the lowest phonon which has a nearly constant frequency, whereas the corresponding peak, clearly resolved, shifts down. Therefore these results are rather artificial. Moreover, as pointed out previously by Tomeno and Matsumara,[4] the dielectric constant as calculated from this model does not reproduce the experimental dielectric data.

V. CONCLUSION

We have studied the temperature dependence of the optical phonons in $LiNbO_3$. Frequency, damping, and oscillator strength have been determined for each A_1 (TO) phonon. At high temperature, the low-frequency A_1 spectrum exhibits the appearance of a quasielastic scattering beside the lowest frequency phonon.

This spectrum has been fitted with a damped harmonic oscillator and a Debye relaxation mode without coupling between them. The A_1 phonon frequency continuously decreases with increasing temperature whereas its damping hugely increases. Extremely anisotropic, the relaxation mode exhibits a critical slowing down characteristic of an order-disorder phase transition.

Our Raman data are able to reproduce the values of the dielectric permittivity along the c axis, as measured at 10 MHz, in the whole temperature range. This remarkable agreement reinforces the confidence in the fitted values and the validity of the interpretation.

*Permanent address: Laboratoire de Physique du Solide, Faculté des Sciences Ben M'Sick, Université Hassan II, Mohamedia, Casablanca, Morocco.

†Electronic mail: bourson@esemetz.ese-metz.fr

[1] W. D. Johnston, Jr. and I. P. Kaminow, Phys. Rev. **168**, 1045 (1968).

[2] A. S. Barker, Jr. and R. Loudon, Phys. Rev. **158**, 433 (1967).

[3] Y. Okamoto, Ping-Chu Wang, and J. F. Scott, Phys. Rev. B **32**, 6787 (1985).

[4] I. Tomeno and S. Matsumara, J. Phys. Soc. Jpn. **56**, 163 (1987).

[5] A. Ridah, P. Bourson, M. D. Fontana, and G. Malovichko (unpublished).

[6] O. F. Schirmer, O. Thiemann, and M. Wöhlecke, J. Phys. Chem. Solids **52**, 185 (1991).

[7] G. I. Malovichko, V. G. Grachev, and O. F. Schirmer, Solid State Commun. **89**, 195 (1994).

[8] B. A. Scott and G. Burns, J. Am. Ceram. Soc. **55**, 225 (1972).

[9] U. Schlarb, S. Klauer, M. Wesselmann, K. Betzler, and M. Wöhlecke, Appl. Phys. A **56**, 311 (1993).

[10] G. E. Kugel, H. Mesli, M. D. Fontana, and D. Rytz, Phys. Rev. B **37**, 5619 (1988).

[11] R. Migoni, H. Bilz, and D. Bäuerle, Phys. Rev. Lett. **37**, 1155 (1976).

[12] P. F. Bordui, R. G. Norwood, D. H. Jundt, and M. M. Fejer, J. Appl. Phys. **71**, 875 (1992).

[13] M. D. Fontana, A. Ridah, G. E. Kugel, and C. Carabatos-Nedelec, J. Phys. C **21**, 5853 (1988).

[14] K. Laabidi, M. D. Fontana, M. Maglione, B. Jannot, and K. A. Muller, Europhys. Lett. **26**, 309 (1994).